

Influence of inter-electrode distance on subthalamic nucleus local field potential recordings in Parkinson's disease



Alberto Averna^a, Sara Marceglia^b, Mattia Arlotti^c, Marco Locatelli^{a,d,e}, Paolo Rampini^{d,e}, Alberto Priori^{a,f}, Tommaso Bocci^{a,f,*}

^a Aldo Ravelli[†] Research Center for Neurotechnology and Experimental Neurotherapeutics, Department of Health Sciences, University of Milan, 20142 Milan, Italy

^b Department of Engineering and Architecture, University of Trieste, 34127 Trieste, Italy

^c Newronika S.r.l., 20093 Cologno Monzese, Italy

^d Department of Neurosurgery, Fondazione IRCCS Cà Granda Ospedale Maggiore Policlinico, Milan, Italy

^e Department of Pathophysiology and Transplantation, University of Milan, Milan, Italy

^f Clinical Neurology Unit I, San Paolo University Hospital, ASST Santi Paolo e Carlo and Department of Health Sciences, 20142 Milan, Italy.

ARTICLE INFO

Article history:

Accepted 5 October 2021

Available online 25 October 2021

Keywords:

Deep brain stimulation

Levodopa

Local field potentials

Phase amplitude coupling

Parkinson's disease

Subthalamic nucleus

HIGHLIGHTS

- Evaluation of differences between subthalamic local field potentials from wide- vs. close-spaced contact pairs, before and after levodopa administration.
- Different spectral and connectivity properties and different correlations with motor symptoms severity between the two contact pairs.
- Findings are relevant to the implementation of better control strategies for adaptive deep brain stimulation.

ABSTRACT

Objectives: To evaluate spectra and their correlations with clinical symptoms of local field potentials (LFP) acquired from wide- and close-spaced contacts (i.e. between contacts 0–3 or LFP03, and contacts 1–2 or LFP12 respectively) on the same DBS electrode within the subthalamus (STN) in Parkinson's disease (PD), before and after levodopa administration.

Methods: LFP12 and LFP03 were recorded from 20 PD patients. We evaluated oscillatory power, local and switched phase-amplitude coupling (l- and Sw-PAC) and correlation with motor symptoms (UPDRSIII).

Results: Before levodopa, both LFP03 and LFP12 power in the α band inversely correlated with UPDRSIII. Differences between contacts were found in the low-frequency bands power. After levodopa, differences in UPDRSIII were associated to changes in LFP03 low- β and LFP12 HFO (high frequency oscillations, 250–350 Hz) power, while a modulation of the low- β power and an increased β -LFO (low frequency oscillations, 15–45 Hz) PAC was found only for LFP12.

Conclusion: This study reveals differences in spectral pattern between LFP12 and LFP03 before and after levodopa administration, as well as different correlations with PD motor symptoms.

Significance: Differences between LFP12 and LFP03 may offer an opportunity for optimizing adaptive deep brain stimulation (aDBS) protocols for PD. LFP12 can be used to detect β -HFO coupling and β power (i.e. bradykinesia), while LFP03 are optimal for low frequency oscillations (dyskinesias).

© 2021 International Federation of Clinical Neurophysiology. Published by Elsevier B.V. This is an open access article under the CC BY-NC-ND license (<http://creativecommons.org/licenses/by-nc-nd/4.0/>).

1. Introduction

The study of local field potentials (LFPs) recorded from the basal ganglia improved the understanding the pathophysiology of

Parkinson's disease (PD) and other movement disorders, leading to the concept of oscillopathy. PD is associated with pathological synchronous oscillatory activity in the subthalamus (STN) in the β band (11–30 Hz range), considered a biomarker for controlling novel DBS approaches (“adaptive DBS”, aDBS) (Arlotti et al., 2018, Giannicola et al., 2012, Levy et al., 2002, Little et al., 2016, Little et al., 2013, Priori et al., 2004, Ray et al., 2008, Rosa et al., 2012).

* Corresponding author.

E-mail address: Tommaso.Bocci@unimi.it (T. Bocci).

LFPs reflect synchronized rhythmic synaptic or neuronal local activities, depending on functional changes occurring in the basal ganglia–cortical network (Brown and Williams, 2005, Hammond et al., 2007). Whereas β oscillations are suppressed by levodopa and correlate with movement preparation and execution (Foffani et al., 2003, Priori et al., 2004), akinesia (Kuhn et al., 2009) and motor imagery (Kuhn et al., 2006a), the low frequency oscillations (i.e. 2–7 Hz) also correlate with dyskinesias (Alonso-Frech et al., 2006, Giannicola et al., 2013, Priori et al., 2004).

Subthalamic LFPs can be also analyzed by phase-amplitude coupling (PAC), a measure that quantify the level of synchronization between the phase of the lower frequency oscillation and the power of the higher frequency oscillation. While oscillatory power is largely an indicator of integrated neuronal synchronization from a localized area (Buzsaki and Watson, 2012), phase-amplitude coupling (PAC) likely reflects local or large-scale inter-network communication subserved through cross-frequency interactions (Jensen and Colgin, 2007). PAC coordinates the timing of neuronal activity and allows to determine the mechanism for communication within distinct functional regions of the STN (López-Azcárate et al., 2010, Ozkurt et al., 2011, van Wijk et al., 2016, Yang et al., 2014).

Despite the correlation of oscillatory power and PAC with PD symptoms (Brittain and Brown, 2014, de Hemptinne et al., 2013, Kuhn et al., 2006b, Kuhn et al., 2009, López-Azcárate et al., 2010, Tsiokos et al., 2017, van Wijk et al., 2016, Weinberger et al., 2009), whether LFP changes are consistent with different electrodes geometry/disposition is still not clear. Yet, no studies have systematically characterized differences between close- and wide-spaced electrode pairs in the subthalamic nucleus. This study aims to evaluate the oscillatory activity, PAC and coherence of STN-LFP captured from close- and wide-spaced electrode pairs in the subthalamic nucleus (STN) of patients with Parkinson’s disease with implanted DBS electrodes.

2. Methods

2.1. Patients

As reported in Table 1, 36 nuclei from 20 patients (10 females and 10 males, of which 4 patients had only unilateral LFPs record-

ings) with Parkinson’s disease were studied after their informed consent and local ethical committee approval (according to Helsinki declaration). Patients underwent functional neurosurgery for bilateral implantation of DBS electrodes in the STN. All of the patients, which had predominantly rigid-akinetic phenotype with severe motor fluctuations, fulfilled national inclusion criteria for DBS treatment (Abbruzzese, 2002). Motor scores were assessed with the Unified Parkinson’s Disease Rating Scale - UPDRS III after surgery (off medication, for patients recorded before levodopa and on medication for patients recorded after levodopa), and motor fluctuations scores (UPDRS IV) before surgery. Localization of STN for DBS recording procedures count on several steps, briefly: the nucleus were identified through pre-operative direct visualization using computed tomography-magnetic resonance imaging (CT-MRI) based targeting (Egidi et al., 2002, Rampini et al., 2003), followed by intra-operative neurophysiology with micro-recordings (Mrakic-Sposta et al., 2008, Priori et al., 2003), intra-operative stimulation (i.e. through the exploratory electrode) and macrostimulation (i.e. through the implanted macroelectrode), and finally post-operative neuroimaging for the final assessment of the electrode position (Egidi et al., 2002, Rampini et al., 2003). The implanted electrode for DBS recordings (Model 3389, Medtronic Inc., Minneapolis, USA) was composed by four metal contacts (1.27 mm in diameter, 1.5 mm in length, spaced 2 mm centre to centre), designated 0–1–2–3 in caudal-rostral direction (see Fig. 1). According to intraoperative and postoperative tests, contact 1 was consistent with placement within the STN, contact 0 denominates the electrode deepest in the STN and electrode 3 the one situated at the interface between the STN and the *zona incerta*. In all patients, the STN-DBS procedures collectively indicated that contact 1–2 was within the STN (Foffani et al., 2003, Marceglia et al., 2006). DBS target stereotactic coordinates and estimated STN length were detailed reported in (Marceglia et al., 2006) and in Supplementary Table S1.

2.2. LFP recordings and experimental protocol

Experimental protocol of this study is composed by two experimental phases and it has been reported in detail elsewhere (Marceglia et al., 2006). Briefly, Post-operative LFPs were recorded three days after surgery, at rest (60–80 s) to avoid the possible

Table 1

Clinical features of patients. Motor scores were assessed with the Unified Parkinson’s Disease Rating Scale - UPDRS III after surgery (off medication, for patients recorded before levodopa and on medication for patients recorded after levodopa), and motor fluctuations scores (UPDRS IV) before surgery.

Patient	Gender	Age (years)	Side	Recording Condition	Levodopa equivalent before surgery (mg)	Dopamine agonist dose before surgery	UPDRSIII Before levodopa	UPDRSIII After levodopa	UPDRSIV Before surgery
1	F	69	R, L	Off, On	1377	3	49	1	11
2	F	55	R, L	Off	1040	2	34.5	5.5	10
3	M	52	R, L	Off	2400	0	66	18.5	9
4	M	66	R, L	Off	975	0.36	44.5	16	10
5	F	61	R, L	Off	925	3	28	10	13
6	M	63	R, L	Off	1260	1.56	37.5	4	-
7	M	59	R, L	Off, On	1800	3	38	4	14
8	F	59	R, L	Off	1671	2.34	28.5	4.4	9
9	F	59	R, L	Off, On	1400	0	49	1	14
10	F	70	R, L	Off, On	1200	1.8	33	2.5	11
11	M	66	R, L	On	900	0.7	44	7.5	14.5
12	M	44	L	Off, On	1500	0	32.5	2	6
13	F	55	R, L	On	1250	3	37.5	4	8
14	F	70	R, L	Off, On	1010	3	36	5.5	11
15	M	56	L	Off, On	2800	14	39	2	12
16	M	38	R, L	Off	3230	5.6	65.5	-	12
17	M	67	R, L	Off	825	2.4	64	17	7
18	M	63	R, L	On	1292	0	11	7	7
19	F	64	R	Off	1995	0	34	9	-
20	F	53	R	Off	900	0	68	21	5

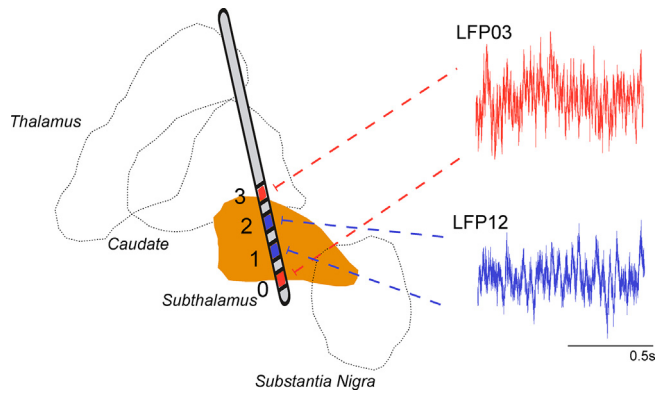


Fig. 1. Deep brain stimulation (DBS) lead and bipolar contact pairs in the Subthalamic nuclei (STN). Figure reports gross anatomy of STN and approximate location of DBS lead. Local field potentials (LFPs) was recorded simultaneously between both close-spaced 1–2 (blue) and wide-spaced 0–3 (red) contact pairs.

influence of movements (passive or active), 12 h after withdrawal of levodopa treatment both before (off medication, 30 nuclei recorded, see Table 1) and after (on medication, 18 nuclei recorded, see Table 1) patients received dopaminergic medication (50–200 mg of oral fast-acting levodopa/benserazide). During the experiment, individual doses of levodopa were adapted to the habitual amount of fast-acting levodopa preparation taken from before surgery, in order to ensure full clinical efficacy. Recordings in the ON condition (after levodopa) were obtained after the evaluation of patient’s clinical conditions performed by an experienced neurologist at least 30 min after medication.

Differential LFP recordings were acquired simultaneously between contacts 1–2 and 0–3 (i.e. LFP12 and LFP03, see Fig. 1) through an analogical amplifier (Signal Conditioner Cambridge 1902, Cambridge Electronic Design, Cambridge, England). The recorded signals were amplified ($\times 100,000$) and filtered (pass-band 2–1000 Hz) then digitized (Cambridge Micro 1402, Cambridge Electronic Design), with sampling rate 2500 Hz and 12-bit quantization with 5 V range.

2.3. LFP analysis

For each patient, two 60 s-long epochs of LFP were extracted at each specific experimental phase (i.e. before and after levodopa). Data were first visually inspected and those sections of data with gross artefacts were removed. To reduce signal variability and ensure matching background noise in all recordings (Foffani et al., 2003, Priori et al., 2004), LFPs were normalized by subtracting the mean and dividing the result by the standard deviation of the 600–1000 Hz band-pass filtered signals. STN oscillations at rest were quantified by LFP power spectral analysis. Data were divided into 15 overlapping and evenly distributed sub-epochs that each comprise 90% of the total length of the original epoch. Data were tapered with a Hanning window and for each sub-epoch, the power spectrum was calculated through Fast Fourier Transform (FFT). The squared magnitudes of each segment were averaged, to obtain the estimated power spectral density (PSD). We analyzed LFPs in the frequency bands that are known to characterize the STN oscillatory pattern, i.e. the δ frequencies (2–4 Hz), θ (4–7 Hz), α (8–12 Hz), low- β (12–20 Hz), high- β (20–30 Hz), low- γ (30–45 Hz) and HFO (250–350 Hz) frequency bands. The spectral power of each frequency band was calculated on all individual nuclei, in patients before and after levodopa, as follows

$$P_{(f_1-f_2)} = \frac{1}{f_2 - f_1} \int_{f_1}^{f_2} PSD(f) df$$

where f_1 and f_2 represent the boundary frequencies of the considered band ($f_1 - f_2$), $P_{(f_1-f_2)}$ is the spectral power in the band ($f_1 - f_2$) and $PSD(f)$ is the PSD at the frequency f .

2.4. Phase amplitude coupling (PAC) analysis

We developed a cross-frequency measure to analyze phase-to-amplitude modulation in our dataset. Phase-to-amplitude comodulograms were constructed by applying modulation index (MI) measure to multiple frequency band pairs (1 Hz bin) made up of “phase frequency” and (5 Hz bin) “amplitude frequency” bands. MI is based on a normalized entropy measure (Hurtado et al., 2004) which has been demonstrated to detect also multimodal phase distributions, using the Nested-Frequency analysis algorithm described in He et al. (He et al., 2010). Phase-amplitude coupling was assessed for every frequency pair in a 2-D frequency space. 1-Hz-width (0.5 steps) frequency bins centered at 2, 3, ..., 40 Hz were used for phase extraction (plotted on x-axis), 5-Hz-width frequency bins centered at 5, 10, ..., 350 Hz were used for amplitude extraction (on y-axis). Briefly, for each frequency pair f_p and f_A , an LFP was filtered in the corresponding frequency bins $[f_p]$ and $[f_A]$ using a 3-order symmetrical Butterworth filter (windows of 60-sec length) after linear-trend removal. Next, instantaneous phase $\phi_{fp}(t)$ and amplitude $A_{fA}(t)$ time series were obtained using standard Hilbert transform. Then the sample-by-sample values of $\phi_{fp}(t)$ were binned into 20 0.1π -width intervals from $-\pi$ to π , and the concurrent $A_{fA}(t)$ values were averaged within each phase bin. An inverted entropy measure H was applied using the mean A_{fA} value at phase bin $\phi_{fp}(j)$ ($j = 1, 2, \dots, 20$).

$$H = - \sum_{j=1}^N p_j \log p_j$$

where $N = 20$ (i.e. number of bins) and p_j is:

$$p_j = \frac{\langle A_{fA} \rangle_{\phi_{fp}(j)}}{\sum_{j=1}^N \langle A_{fA} \rangle_{\phi_{fp}(j)}}$$

The modulation index (MI), which describes the deviation of $\langle A_{fA} \rangle_{\phi_{fp}(j)}$ from a uniform distribution (Tort et al., 2008), is obtained by normalizing H by the maximum possible entropy value ($H_{max} = \log N$, where $N = 20$) as:

$$MI = \frac{H_{max} - H}{H_{max}}$$

Thus, a low MI indicates lack of phase-to-amplitude modulation (i.e., $\langle A_{fA} \rangle_{\phi_{fp}(j)}$ constant for all phase bins), and larger MI values result from stronger phase-to-amplitude modulation.

MI was calculated both locally (i.e. LFP12-LFP12 and LFP03-LFP03) and by switching phase and amplitude from the two locations (i.e. LFP12-LFP03 and LFP03-LFP12), denoted respectively l-PAC and Sw-PAC. To assess the statistical significance of the MI values, this was compared against a distribution of 44 shuffled time series (obtained by cutting $\phi_{fp}(t)$ in 5 segments of the same length and then shuffling them with no repetition), by using a shuffling procedure which preserves the temporal structure of the original signal (He et al., 2010, Hurtado et al., 2004). A Z-score statistic for MI was finally obtained by comparing the original values against the means and the standard deviation of the shuffled MI. The phase-amplitude combinations which visually showed the greatest Z-scores, namely β -HFO (i.e. phase in the range 12–30 Hz and amplitude 250–350 Hz) and β -LFO (i.e. phase in the range 12–30 Hz and amplitude 15–45 Hz), were considered for statistics.

2.5. Envelope imaginary coherence (EIC)

In order to measure frequency-specific synchronization between LFP12 and LFP03, we implemented an iCOH-derived measure, the envelope of the imaginary coherence (EIC) operator as described in (Sanchez Bornot et al., 2018) which suppose not to be affected by volume conduction. EIC is calculated as the absolute value of the analytical signal estimated from the iCOH function (Nolte et al., 2004) in the frequency domain. Contrarily to iCOH, which heavily relies on the imaginary part while directly ignoring any useful information contained in the real part, EIC method has been demonstrated to partially recover that information, thus showing superior results.

2.6. Statistical analysis

To investigate levodopa effect on both power spectral and coherence analysis, we first checked for normality of distribution with Shapiro-Wilk test prior to comparing scores between before and after levodopa conditions since our sample size is < 50 . Since the normality condition was not satisfied, non-parametric paired sample Wilcoxon signed-rank test of equality of medians (Matlab function “signrank”) was applied ($p < 0.05$).

To determine significant differences between LFPs paired contacts (recorded from close LFP12 and wide LFP03 contacts), a repeated-measures analysis of variance (ANOVA, “fitrm”) was performed to the subset of patients that were recorded both in off and in on levodopa condition (12 nuclei from 7 patients). With both pairs of contacts (i.e. 1–2 and 0–3) and treatment (i.e. before and after levodopa) as a grouping factor (within-subject factors) and different frequency bands as between factor. Tukey–Kramer post-hoc test was used to identify significant contacts-related differences estimating the error variance for independent measures in individual bands ($p < 0.05$).

For PAC analysis, statistical significance of MI Z-score was evaluated using conventional Z-to-P transform after controlling for multiple comparisons using Bonferroni correction. Each nucleus was considered as individual sample and an analysis of variance for unbalanced data was calculated for the entire cohort of Z-scores (36 nuclei from 20 patients) through the Matlab function “anovan”, considering as grouping factors: the treatments (i.e. before and after levodopa), the phase-amplitude combinations and the different contacts (i.e. 03 and 12). Significant differences

were computed using the “multcompare” function with Bonferroni post-hoc analysis.

For Coherence analysis, the significance of EIC values were determined by a threshold curve which was computed using the maximum (minimum) value statistics of EIC values obtained from surrogate data (Lachaux et al., 1999). We used 1000 randomized samples in our simulation and computed this statistic for each frequency, separately.

The SPSS © version 27 statistical package (SPSS Inc., Chicago, Ill., USA) was used to compute the correlation between both UPDRSIII and UPDRSIV scores and the spectral power of LFP recordings from the different contacts using Pearson’s coefficient with bootstrap validation technique for estimation of 95% confidence intervals CIs (1000 bootstrap samples).

3. Results

3.1. LFP12, LFP03 power spectral density (PSD)

During baseline period of recording (i.e. before levodopa), both LFP12 and LFP03 spectra were characterized by oscillatory activity below 30 Hz, particularly in the low- β (12–20 Hz) and high- β range (20–30 Hz), while there was no spectral peak in the gamma range.

As shown in Fig. 2, power spectra differed between LFP12 and LFP03. Before levodopa, in comparison to LFP12, LFP03 had higher power in δ (2–4 Hz), θ (4–7 Hz) and α (7–12 Hz) bands, while lower power in HFO (250–350 Hz) (Table 2). After Levodopa, differences between LFP12 and LFP03 changed: LFP03 power in δ (2–4 Hz), θ (4–7 Hz), α (7–12 Hz) and low- β (12–20 Hz) was greater than LFP12, while it was lower in HFO (250–350 Hz) (Table 2).

Levodopa induced changes in both LFP12 and LFP03 power spectra in comparison to their baseline pattern before the drug. LFP12 PSD after levodopa showed a reduction in the low- β band (12–20 Hz) (Wilcoxon signed-rank test *, $p = 0.026$) and an increase of the HFO (250–350 Hz) (Wilcoxon signed-rank test *, $p = 0.012$) respect to before levodopa. LFP03 PSD increased after levodopa in the δ (2–4 Hz) band in comparison to before levodopa (Wilcoxon signed-rank test *, $p < 0.001$) (Fig. 2).

3.2. Correlation between signal power and motor symptoms

Before levodopa, the α power of both LFP03 and LFP12 inversely correlated with the pre-treatment motor UPDRSIII score

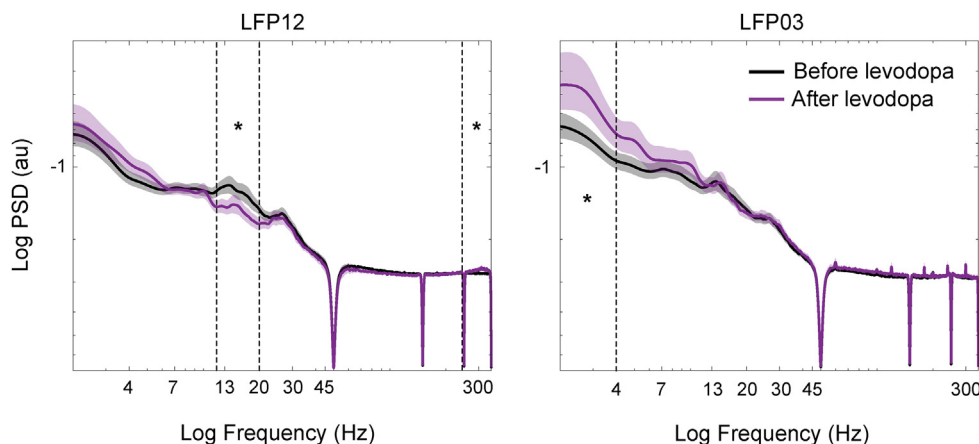


Fig. 2. Grand averaged Power Spectral Density (PSD) for local field potentials (LFPs) between close (LFP12, left) and wide (LFP03, right) spaced contact pairs in log space during each experimental phase (i.e. before levodopa and after levodopa). The x-axis reports frequencies (Hz), plotted on a logarithmic scale between 2 and 350 Hz; the y-axis shows PSD values, expressed in logarithmic arbitrary units (AU). Note the decrease of LFP12 Low- β (12–20 Hz) and increase of both LFP12 high frequency oscillations (HFO, 250–350 Hz) and LFP03 δ (2–4 Hz) spectral power after levodopa. * = statistical significance of the difference between the two conditions as tested by Wilcoxon signed-rank test ($P < 0.05$).

Table 2

Details of levodopa-induced changes on local field potential (LFP) bands spectral power, in both close (LFP12) and wide (LFP03) spaced contact pairs recorded both before and after levodopa (12 nuclei from 7 subjects).

TestCond	Contacts	Difference	StdErr	pValue	Lower	Upper
δ Off	03 vs 12	0,3077	0,0882	0,0051*	0,1135	0,5019
δ On		0,3369	0,1144	0,0134*	0,0850	0,5887
θ Off		0,4364	0,0914	0,0006*	0,2351	0,6376
θ On		0,3790	0,1111	0,0058*	0,1344	0,6235
α Off		0,2951	0,0825	0,0043*	0,1136	0,4766
α On		0,3710	0,0884	0,0015*	0,1764	0,5656
Low- β Off		0,0807	0,0916	0,3971	-0,1209	0,2822
Low- β On		0,2958	0,0797	0,0034*	0,1205	0,4712
High- β Off		-0,0044	0,0752	0,9544	-0,1699	0,1611
High- β On		0,0766	0,0482	0,1399	-0,0294	0,1826
Low- γ Off		-0,0577	0,0530	0,2991	-0,1743	0,0589
Low- γ On		0,0598	0,0561	0,3095	-0,0637	0,1833
HFO Off		-0,1664	0,0711	0,0392*	-0,3230	-0,0099
HFO On		-0,2251	0,0557	0,0019*	-0,3476	-0,1025

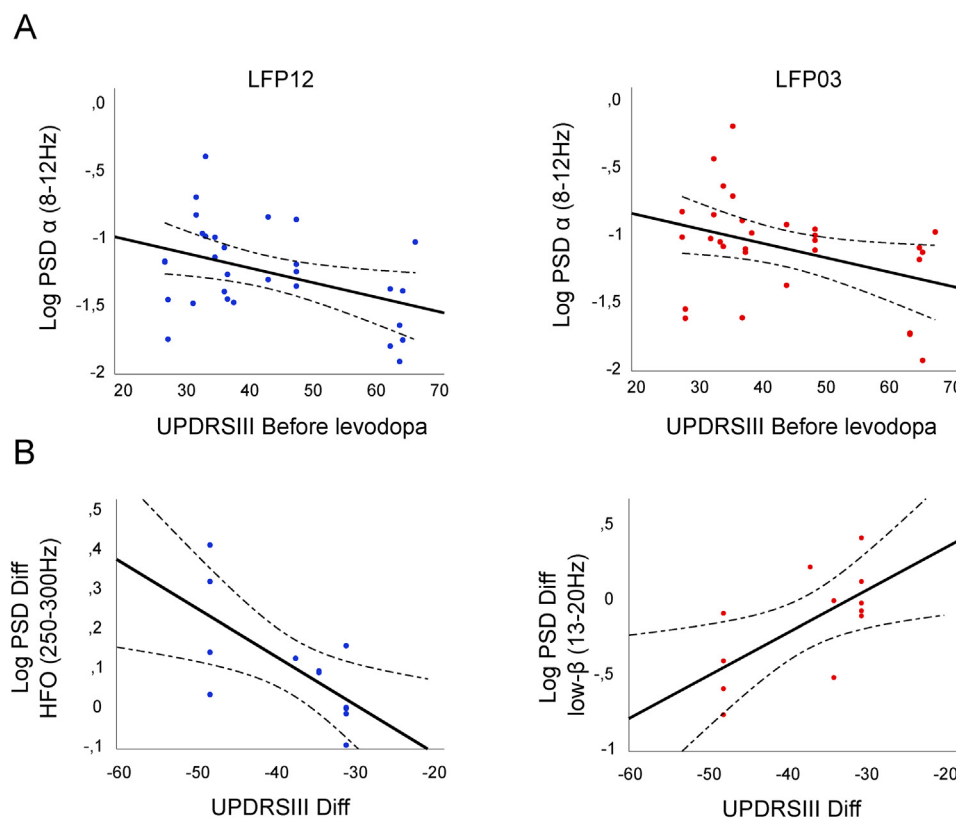


Fig. 3. Correlation plots showing associations between UPDRSIII score and α power Before levodopa (A) and between treatment induced changes of high frequency oscillations (HFO) power and changes in UPDRSIII (i.e. before levodopa – after levodopa, B). Note that patients with lower motor impairment had the higher level of both close spaced (LFP12) and wide spaced local field potentials LFP03 α (8–12 Hz) power ($r = -0.409$, p -value = 0.034 and $r = -0.415$, p -value = 0.032, respectively, panel A). Patients with the best improvement of motor symptoms after levodopa had the higher increase of LFP12 HFO (250–350 Hz) and the higher decrease of LFP03 low- β (12–20 Hz) power ($r = -0.672$, p -value = 0.017 and $r = 0.650$, p -value = 0.022 respectively, panel B).

($r = -0.415$, p -value = 0.032, 95% CI [-0.717, -0.41] and $r = -0.409$, p -value = 0.034, 95% CI [-0.714 -0.025] respectively) (Fig. 3). After levodopa, the increase of HFO power in LFP12 (i.e. before levodopa – after levodopa) negatively correlated ($r = -0.672$, p -value = 0.017, 95% CI [-0.949, -0.136]) with the improvement of UPDRSIII score (i.e. UPDRSIII before levodopa – UPDRSIII after levodopa). Levodopa-induced motor improvement positively correlated to LFP03 variations in low- β band ($r = 0.650$, p -value = 0.022, 95% CI [0.200, 0.887]). Furthermore, we did not find any correlation between motor fluctuations, assessed before surgery (UPDRS IV score), and both LFP03 and LFP12 power variations in all the frequency bands (data not shown).

3.3. Local and switched PAC

Before levodopa, LFP12 showed a strong β -HFO PAC (Fig. 4A, top), while after levodopa β -LFO coupling increased (*, $p = 0.013$) and β -HFO decreased (* $p < 0.0001$) with respect to before levodopa (Fig. 4B). LFP03 also showed a marked β -HFO PAC before levodopa (Fig. 4A, bottom), and after levodopa we found a decrease in β -HFO PAC (* $p < 0.0001$) in comparison to before levodopa condition (Fig. 4B).

PAC differed between LFP12 and LFP03. Either before and after levodopa LFP03 had lower level of β -LFO and β -HFO coupling than LFP12 (Fig. 4B, o, $p < 0.0001$).

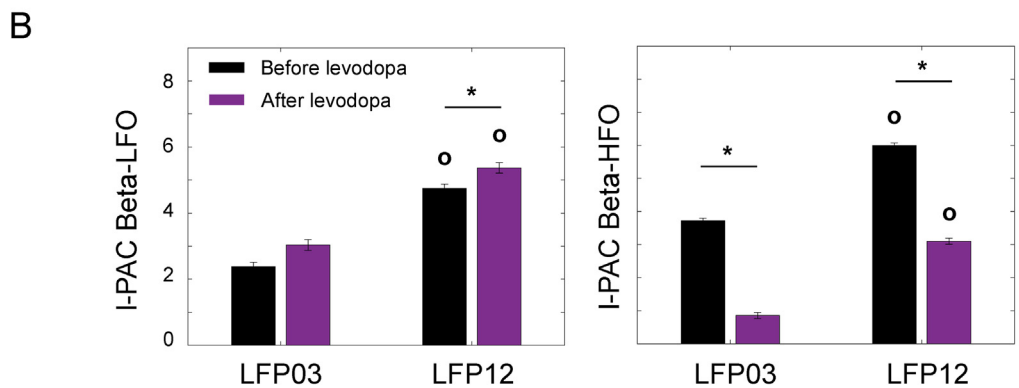
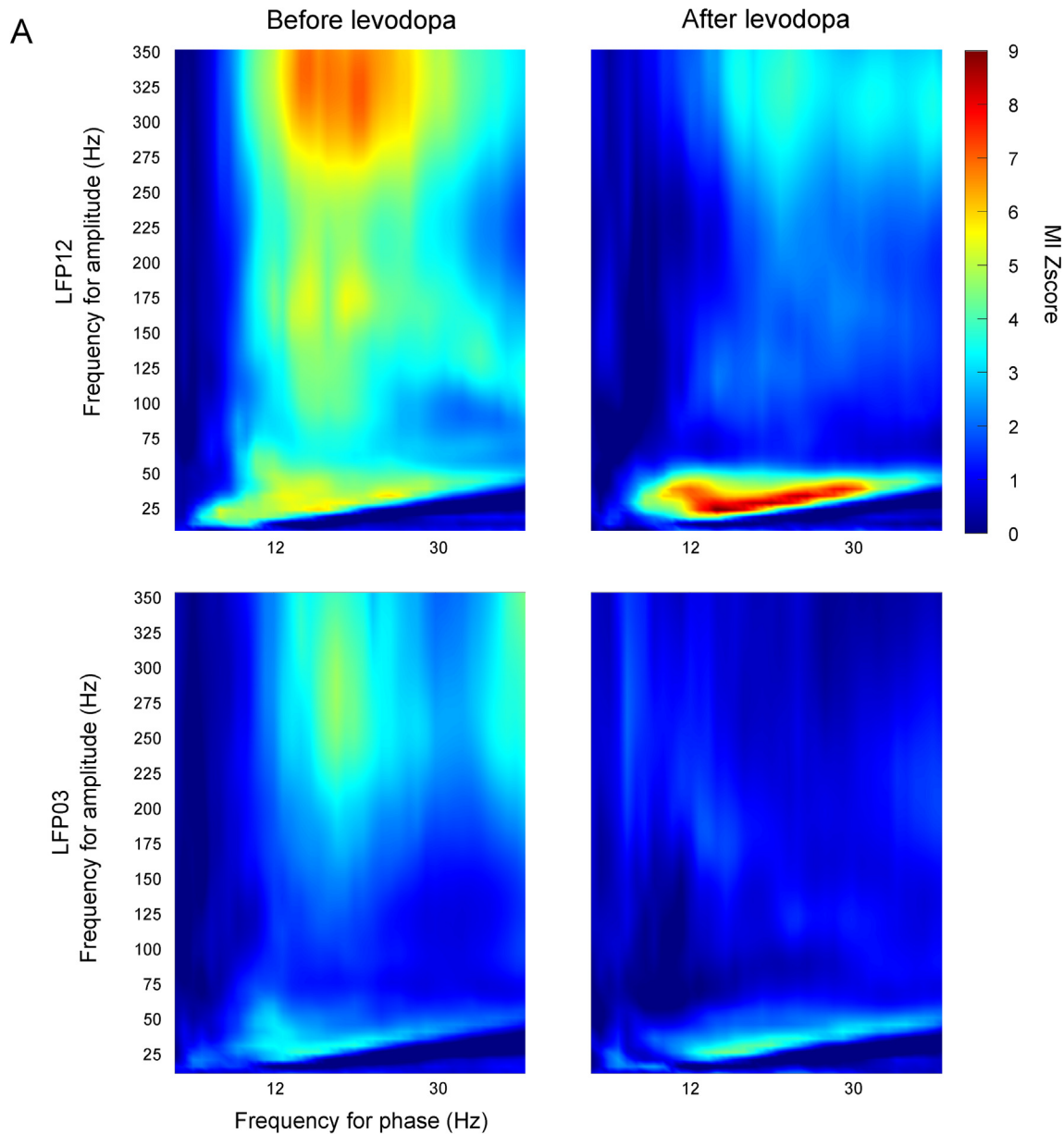


Fig. 4. Subthalamic nuclei (STN) local phase-amplitude coupling (I-PAC): spatial distribution and pharmacological modulation. A) Averaged I-PAC comodulograms (Bonferroni corrected MI Z-values) for the cohort of close spaced (LFP12, top) and wide spaced local field potentials (LFP03, bottom), before levodopa (left) and after levodopa (right). B) Comparison of average PAC values at different frequency bands during before levodopa (black) and after levodopa (purple) indicates both significant suppression of the β -high frequency oscillations (β -HFO) I-PAC for both the groups and increase of the β -low frequency oscillations (β -LFO) I-PAC only for LFP12. Asterisk signs (*) indicate statistical significance of the difference between the two conditions as tested by multiple comparison procedure using Bonferroni method $p < 0.0001$. Circle signs (o) indicate statistical significance of the difference between the two groups (i.e. LFP12 and LFP03) as tested by multiple comparison procedure using Bonferroni method $p < 0.0001$. Note that levodopa decreased the strong LFP12 and LFP03 β -HFO I-PAC found before levodopa but increased LFP12 β -LFO I-PAC.

Before levodopa there was a strong Sw-PAC between LFP12 HFO amplitude and LFP03 β phase (Fig. 5A, β -HFO Sw-PAC0312). Conversely, after levodopa Sw-PAC between LFP03 LFO amplitude and LFP12 phase increased (β -LFO Sw-PAC0312, *, $p < 0.0001$) with respect to before levodopa.

Before levodopa, β -LFO Sw-PAC0312 was greater than β -LFO SwPAC1203 (Fig. 5B, o, $p < 0.0001$). After levodopa, β -LFO Sw-PAC0312 again was greater than β -LFO SwPAC1203 but β -HFO Sw-PAC0312 was lower than β -HFO Sw-PAC1203 (Fig. 5B, o, $p < 0.0001$).

3.4. LFP12-LFP03 coherence

Before levodopa, LFP12 and LFP03 in the same STN correlated in the low- β (12–20 Hz) band (Fig. 6A) with a significant peak at 13.43 Hz (± 1.78). After levodopa the synchrony between LFP12 and LFP03 in the low- β band decreased ($p = 0.0097$, Wilcoxon signed-rank test).

4. Discussion

The main finding is that STN-LFP differ between close- (LFP12) and large-spaced (LFP03) electrode recordings.

Before levodopa, whereas the low- β (12–20 Hz) band did not differ between the two pairs of contacts (LFP12 and LFP03), δ , θ and α bands had higher power in wide-spaced contacts recordings (LFP03) than in close-spaced pairs (LFP12). After levodopa, low- β PSD decreased only in LFP12. Hence, whereas LFP12 are more informative for β -rhythm controlled aDBS (e.g. for sensing bradykinesia), LFP03 seem more suitable for low-frequency controlled aDBS approaches (e.g. for detection of dyskinesias).

In this study we did not systematically evaluate the post-operative position through reconstruction of each lead into the STN. Nevertheless, the placement of closed spaced contacts (1–2) was verified to be within the STN, according to intraoperative and postoperative tests (Foffani et al., 2003, Marceglia et al., 2006, Priori et al., 2004), thus suggesting that wide spaced contacts (0–3) were placed near the borders of STN. Moreover, the main objective of our study was to investigate the characteristic of the signals captured by DBS probes commonly used in clinical practice when positioned within the subthalamus at the most effective location for the treatment, as well as the differences between potentials recorded with closely- and largely spaced pair of contacts.

Greater low-frequency power in wide-spaced electrodes before levodopa could arise from larger distance between contacts: greater interelectrode distance increases the signal magnitude by capturing the activity of more distant neurons (Kent and Grill, 2014, Lempka and McIntyre, 2013). δ frequency (2–4 Hz) STN increase after levodopa is further enhanced in LFP03. In STN-LFP recordings low-frequency oscillations have already been shown to be present before levodopa (Priori et al., 2006, Priori et al., 2004) and to increase following dopaminergic medication (Alonso-Frech et al., 2006, Priori et al., 2004, Silberstein et al., 2003). Furthermore, changes in low-frequency power, intended as 2–7 Hz power band, has been shown to be associated to the increase of the electrode impedance after levodopa intake, thus positively correlating with patient's clinical improvement (Giannicola et al., 2013). Thus, since the electrode impedance increases 30 days after surgery (Rosa et al., 2010), the low frequency modulation, as the time elapsing after DBS surgery lengthens, could be even more pronounced and useful as a control signal for aDBS.

The correlation between baseline UPDRSIII values and α power is a novel finding. Subthalamic α oscillations are known to corre-

late both with executive and limbic functions, as well as with gait speed (Alonso-Frech et al., 2006) and dyskinesias (7.5–11.0 Hz) (Rodriguez-Oroz et al., 2011). From a functional point of view, α oscillations are related to a dysfunctional circuitry connecting the STN with premotor and prefrontal areas (Horn et al., 2017), possibly underlying the generation of the freezing of gait (Dagan et al., 2017, Kostic et al., 2012, Vercruyssen et al., 2014). Previous studies did not emphasize the correlation between baseline UPDRSIII and power in the α band, probably because α frequencies are often considered within the β range. Another possibility is that different subthalamic oscillations have predominant spatial locations and α frequencies seem to be confined in the anterior portion of the nucleus (Horn et al., 2017), even if (Kühn et al., 2005) using directional electrodes (Bour et al., 2015) the topography of the < 10 Hz band LFP activity was more distributed and variable than the activity in the 11–40 Hz band. Recordings with directional electrodes suggest that also beta oscillations may have a more widespread origin than previously thought, including the ventral STN and the substantia nigra *pars reticulata* (SNr) (Alavi et al., 2013, Wang et al., 2017).

Consistently with previous studies (Foffani et al., 2003, Marceglia et al., 2006), we found no relationship between presurgery UPDRS IV scores, which establish the severity of motor fluctuations, and oscillatory activities recorded from both wide and close-spaced contact pairs. This suggests that levodopa-induced changes of LFP power in our data might not be attributable to the level of dyskinesia and fluctuations of each patient before the surgery.

Despite levodopa reduced coherence between LFP12 and LFP03 and changed the power of low- β band in LFP12, only differences in the low- β band for LFP03 were positively correlated to the UPDRS improvement. The correlation might be explained by the interaction among different oscillatory networks within the basal ganglia motor circuits or to the interplay between STN, GPe and motor cortex (Bevan et al., 2002), rather than the STN alone. This is a new finding, strengthening the hypothesis that beta oscillations do not have a specifically topographic localization within the dorsal subthalamus, but may originate from a wide dysfunctional network outside the STN, including also the SNpr, thus driving both the motor input and output from the STN (Alavi et al., 2013, Brazhnik et al., 2012, Haumesser et al., 2021, Sutton et al., 2013, Wang et al., 2017); nonetheless, whether beta oscillations share the same anatomical generator for all these recording sites is still to be elucidated.

We provide also novel data about the effects of dopaminergic modulation on PAC. Levodopa reduces the coupling between β and high-frequency oscillations (HFO), increasing at the same time PAC between β and low-frequency oscillations (LFO). Though we found these changes both in LFP12 and LFP03, they were greater for LFP12. We found a levodopa-induced suppression of β -HFO (50–350 Hz) coupling, which is in agreement with the observed correlation with the severity of motor impairment and bradykinesia (López-Azcárate et al., 2010, van Wijk et al., 2016), likely depending upon the greater duration of STN β bursts (Sanders, 2016) before levodopa administration (Brittain et al., 2014, de Hemptinne et al., 2015, Eusebio and Brown, 2009, Salimpour and Anderson, 2015, Tsiokos et al., 2017), despite not measured in this study.

Apart from the oscillatory activity, we also assessed the PAC between different frequencies. PAC reflects whether and how different frequency bands, spoken by different neuronal populations or basal ganglia networks, interact each other. It has already been demonstrated that β phase- high frequency (200–500 Hz) amplitude coupling is present in subcortical structure such as the STN (Ozkurt et al., 2011, Yang et al., 2014) and it correlates with severity of motor impairment in PD (van Wijk et al., 2016). In particular,

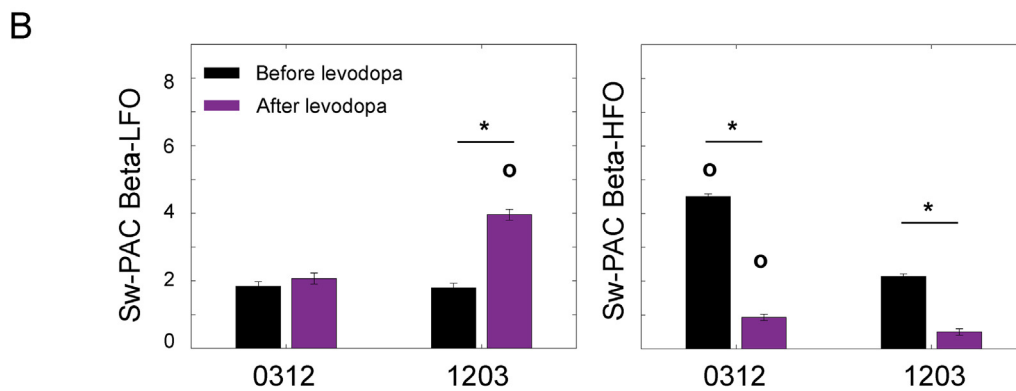
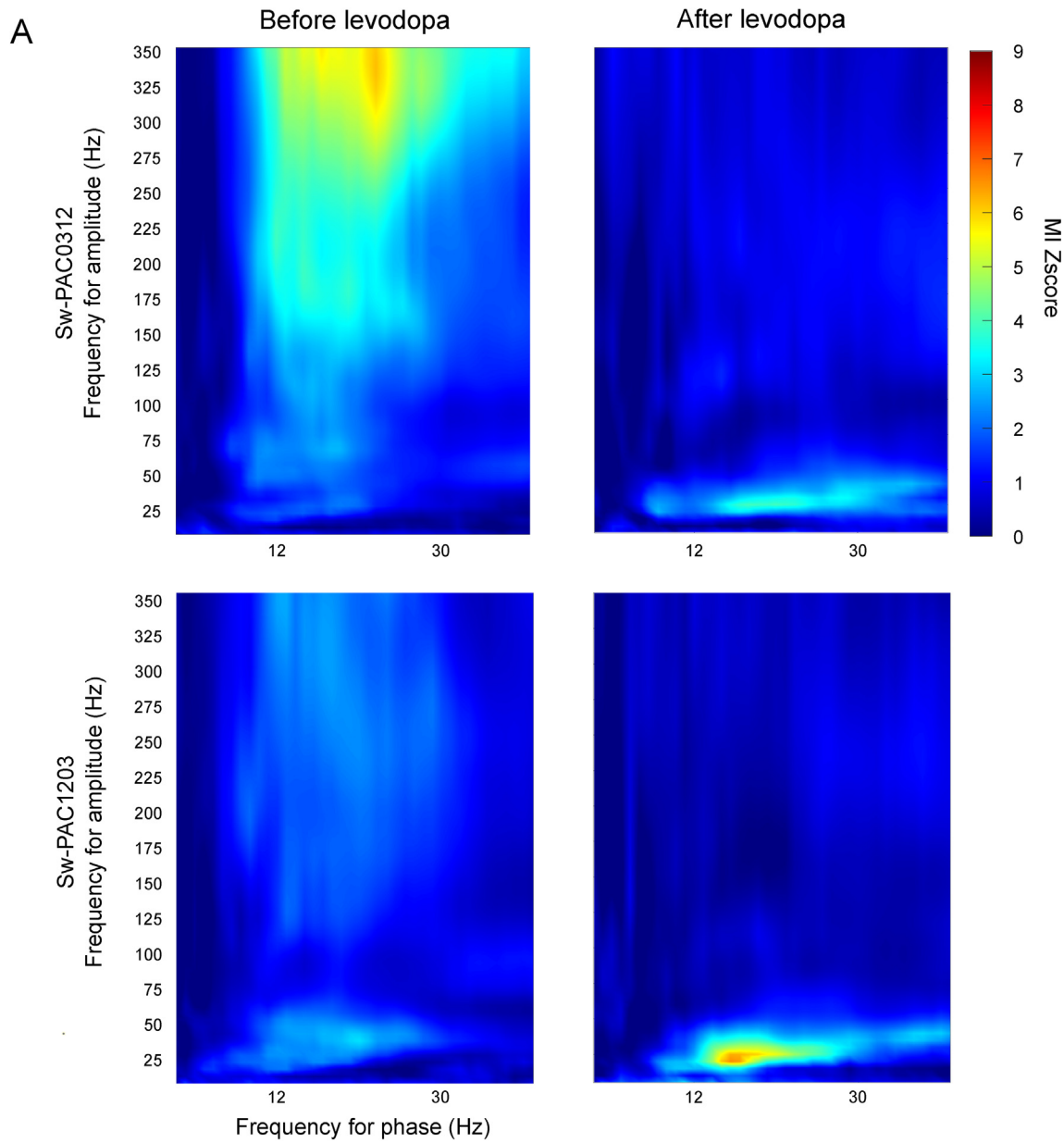


Fig. 5. Switched Subthalamic nuclei (STN) phase-amplitude coupling (Sw-PAC): spatial distribution and pharmacological modulation. A) Averaged Sw-PAC comodulograms (Bonferroni corrected MI Z-values) for the cohort of close spaced (LFP12, top) and wide spaced local field potentials (LFP03, bottom), before levodopa (left) and after levodopa (right). B) Comparison of average PAC values at different frequency bands before levodopa (black) and after levodopa (purple) indicates both significant suppression of the β -high frequency oscillations (β -HFO) Sw-PAC for both the groups (i.e. PAC0312 and PAC1203) and increase of β -low frequency oscillations (β -LFO) Sw-PAC only for PAC1203. * difference between the two conditions $p < 0.0001$. o: difference between the two groups (i.e. PAC0312 and PAC1203) $p < 0.0001$. Note that levodopa decreased the β -HFO Sw-PAC0312 found before levodopa but increased β -LFO Sw-PAC1203.

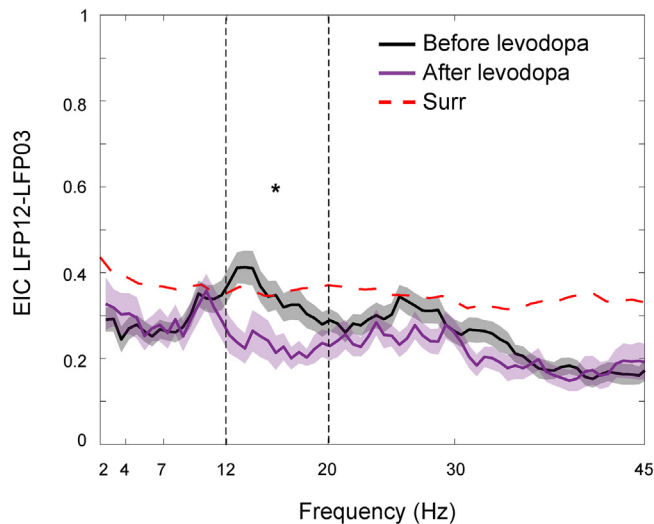


Fig. 6. The envelope of the imaginary coherence (EIC) as a measure of coherence between close spaced (LFP12) and wide spaced local field potentials (LFP03) before levodopa (black line) and after levodopa (purple line). Bold lines are the mean and shaded areas represent the SD. *: $P < 0.05$. Red dotted line represents surrogate based statistics. Note that peak coherence at 13.43 Hz (± 1.78) before levodopa was significantly suppressed after drug administration.

the levodopa-induced modulation of β -LFO (15–45 Hz) coupling for both LFP12 and LFP03 is a novel finding. Low- γ oscillations correlate with the severity of tremor in PD (Beudel et al., 2015, Weinberger et al., 2009). In this view, “prokinetic” low- γ activity may counteract by inhibiting β oscillations during voluntary movements (Florin et al., 2013). In fact, low- β -low- γ PAC is a normal mechanism by which a pro-kinetic rhythm is controlled in the GPi (Tsiokos et al., 2017), possibly accounting the increased β -LFO coupling found in STN following dopaminergic stimulation.

Whereas PAC has been mainly used with one signal, we applied PAC to two LFP signals to infer the direction and strength of rhythmic neural transmission between distinct neuronal networks (Nandi et al., 2019). The hypothesis that justifies such measure is based on the evidence that γ components of LFPs are generated by transmembrane currents related to action potentials (Ray and Maunsell, 2011, Watson et al., 2018). PAC calculated between the amplitude of γ (>30 Hz, in this case both LFO and HFO) in one LFP (e.g. LFP12) and the phase of a low-frequency oscillation (12–30 Hz, β in this case) in another (e.g. LFP03), referred to switched PAC (Sw-PAC) here, would therefore relate the output (spiking detected from LFP12) of one area to the input (somatic/dendritic postsynaptic potentials captured from LFP03) of the other (Nandi et al., 2019). We found that before levodopa, HFO amplitude of LFP12 was significantly coupled to β phase of LFP03 but not vice versa, suggesting the direction of neural transmission (i.e. input \rightarrow output) LFP12 \rightarrow LFP03. Levodopa reduced coupling between HFO amplitude and β phase, but it increased synchrony between LFO amplitude of LFP03 and β phase of LFP12, suggesting the opposite direction of neural transmission (i.e. LFP03 \rightarrow LFP02) but somehow throughout different mechanism. The identification of these “drivers” in the neuronal network, e.g., contact pairs showing strongest Sw-PAC and connectivity, could represent a basis for the spatial specificity of DBS.

5. Conclusions

STN-LFP recorded from wide- (LFP03) and close- (LFP12) spaced contacts before and after levodopa have different spectral and con-

nectivity properties, and differently correlate to the severity of motor impairment.

Differences between LFP12 and LFP03 reflect the contribution of both local and distant neural populations. Smaller contact-to-contact spacing are more sensitive to local oscillations, while larger spacing is strongly influenced by oscillations generated from remote neuronal processes.

Levodopa administration differently affects these oscillations, suggesting a broader effect on the basal ganglia motor circuit whose neural mechanism might be therefore better assessed by wide-spaced contacts.

The results of our study prove that close-spaced contact pairs are optimal for the detection of both β -HFO coupling and β power (i.e. for sensing bradykinesia), while wide spaced contact pairs are more indicated for the detection of low frequency oscillations (dyskinesias). This finding may have important implications for the emerging field of closed-loop adaptive stimulation in PD (i.e. aDBS), thus promoting novel potential sources of control signal for closed-loop stimulation.

Funding

AA and TB were supported by the Aldo Ravelli Research Center for Neurotechnology and Experimental Neurotherapeutics.

Declaration of Competing Interest

The authors declare that they have no known competing financial interests or personal relationships that could have appeared to influence the work reported in this paper.

Appendix A. Supplementary data

Supplementary data to this article can be found online at <https://doi.org/10.1016/j.clinph.2021.10.003>.

References

- Linee AG. Guida per il trattamento della Malattia di Parkinson 2002. Bristol-Myers Squibb; 2002.
- Alavi M, Dostrovsky JO, Hodaie M, Lozano AM, Hutchison WD. Spatial extent of beta oscillatory activity in and between the subthalamic nucleus and substantia nigra pars reticulata of Parkinson's disease patients. *Exp Neurol* 2013;245:60–71.
- Alonso-Frech F, Zamarbide I, Alegre M, Rodriguez-Oroz MC, Guridi J, Manrique M, et al. Slow oscillatory activity and levodopa-induced dyskinesias in Parkinson's disease. *Brain* 2006;129:1748–57.
- Arlotti M, Marceglia S, Foffani G, Volkmann J, Lozano AM, Moro E, Cogiamanian F, Prenassi M, Bocci T, Cortese F, Rampini P, Barbieri S, Priori A. Eight-hours adaptive deep brain stimulation in patients with Parkinson disease. *Neurology* 2018;90(11):e971–6.
- Beudel M, Little S, Pogosyan A, Ashkan K, Foltynie T, Limousin P, Zrinzo L, Hariz M, Bogdanovic M, Cheeran B, Green AL, Aziz T, Thevathasan W, Brown P. Tremor reduction by deep brain stimulation is associated with gamma power suppression in Parkinson's disease. *Neuromodulation* 2015;18(5):349–54.
- Bevan MD, Magill PJ, Terman D, Bolam JP, Wilson CJ. Move to the rhythm: oscillations in the subthalamic nucleus-external globus pallidus network. *Trends Neurosci* 2002;25(10):525–31.
- Bour LJ, Lourens MAJ, Verhagen R, de Bie RMA, van den Munckhof P, Schuurman PR, Contarino MF. Directional recording of subthalamic spectral power densities in Parkinson's disease and the effect of steering deep brain stimulation. *Brain Stimul* 2015;8(4):730–41.
- Brazhnik E, Cruz AV, Avila I, Wahba MI, Novikov N, Ilieva NM, McCoy AJ, Gerber C, Walters JR. State-dependent spike and local field synchronization between motor cortex and substantia nigra in hemiparkinsonian rats. *J Neurosci* 2012;32(23):7869–80.
- Brittain J-S, Brown P. Oscillations and the basal ganglia: motor control and beyond. *Neuroimage* 2014;85:637–47.
- Brittain J-S, Sharott A, Brown P. The highs and lows of beta activity in cortico-basal ganglia loops. *Eur J Neurosci* 2014;39(11):1951–9.
- Brown P, Williams D. Basal ganglia local field potential activity: character and functional significance in the human. *Clin Neurophysiol* 2005;116(11):2510–9.

- Buzsaki G, Watson BO. Brain rhythms and neural syntax: implications for efficient coding of cognitive content and neuropsychiatric disease. *Dialogues Clin Neurosci* 2012;14(4):345–67.
- Dagan M, Herman T, Mirelman A, Giladi N, Hausdorff JM. The role of the prefrontal cortex in freezing of gait in Parkinson's disease: insights from a deep repetitive transcranial magnetic stimulation exploratory study. *Exp Brain Res* 2017;235(8):2463–72.
- de Hemptinne C, Ryapolova-Webb ES, Air EL, Garcia PA, Miller KJ, Ojemann JG, Ostrem JL, Galifianakis NB, Starr PA. Exaggerated phase-amplitude coupling in the primary motor cortex in Parkinson disease. *Proc Natl Acad Sci U S A* 2013;110(12):4780–5.
- de Hemptinne C, Swann NC, Ostrem JL, Ryapolova-Webb ES, San Luciano M, Galifianakis NB, Starr PA. Therapeutic deep brain stimulation reduces cortical phase-amplitude coupling in Parkinson's disease. *Nat Neurosci* 2015;18(5):779–86.
- Egidi M, Rampini P, Locatelli M, Farabola M, Priori A, Pesenti A, et al. Visualisation of the subthalamic nucleus: a multiple sequential image fusion (MuSIF) technique for direct stereotaxic localisation and postoperative control. *Neurol Sci* 2002;23 Suppl 2(2):S71–2.
- Eusebio A, Brown P. Synchronisation in the beta frequency-band—the bad boy of parkinsonism or an innocent bystander? *Exp Neurol* 2009;217(1):1–3.
- Florin E, Dafsari HS, Reck C, Barbe MT, Pauls KA, Maarouf M, et al. Modulation of local field potential power of the subthalamic nucleus during isometric force generation in patients with Parkinson's disease. *Neuroscience* 2013;240:106–16.
- Foffani G, Priori A, Egidi M, Rampini P, Tamma F, Caputo E, et al. 300-Hz subthalamic oscillations in Parkinson's disease. *Brain* 2003;126:2153–63.
- Giannicola G, Rosa M, Marceglia S, Scelzo E, Rossi L, Servello D, Menghetti C, Pacchetti C, Zangaglia R, Locatelli M, Caputo E, Cogliamariani F, Ardolino G, Barbieri S, Priori A. The effects of levodopa and deep brain stimulation on subthalamic local field low-frequency oscillations in Parkinson's disease. *Neurosignals* 2013;21(1–2):89–98.
- Giannicola G, Rosa M, Servello D, Menghetti C, Carrabba G, Pacchetti C, Zangaglia R, Cogliamariani F, Scelzo E, Marceglia S, Rossi L, Priori A. Subthalamic local field potentials after seven-year deep brain stimulation in Parkinson's disease. *Exp Neurol* 2012;237(2):312–7.
- Hammond C, Bergman H, Brown P. Pathological synchronization in Parkinson's disease: networks, models and treatments. *Trends Neurosci* 2007;30(7):357–64.
- Hauemesser JK, Beck MH, Pellegrini F, Kühn J, Neumann W-J, Altschüler J, Harnack D, Kupsch A, Nikulin VV, Kühn AA, van Riesen C. Subthalamic beta oscillations correlate with dopaminergic degeneration in experimental parkinsonism. *Exp Neurol* 2021;335:113513. <https://doi.org/10.1016/j.expneurol.2020.113513>.
- He BJ, Zempel JM, Snyder AZ, Raichle ME. The temporal structures and functional significance of scale-free brain activity. *Neuron* 2010;66(3):353–69.
- Horn A, Neumann WJ, Degen K, Schneider GH, Kuhn AA. Toward an electrophysiological “sweet spot” for deep brain stimulation in the subthalamic nucleus. *Hum Brain Mapp* 2017;38(7):3377–90.
- Hurtado JM, Rubchinsky LL, Sigvardt KA. Statistical method for detection of phase-locking episodes in neural oscillations. *J Neurophysiol* 2004;91(4):1883–98.
- Jensen O, Colgin LL. Cross-frequency coupling between neuronal oscillations. *Trends Cogn Sci* 2007;11(7):267–9.
- Kent AR, Grill WM. Analysis of deep brain stimulation electrode characteristics for neural recording. *J Neural Eng* 2014;11(4):046010. <https://doi.org/10.1088/1741-2560/11/4/046010>.
- Kostic VS, Agosta F, Pievani M, Stefanova E, Jecmenica-Lukic M, Scarale A, Spica V, Filippi M. Pattern of brain tissue loss associated with freezing of gait in Parkinson disease. *Neurology* 2012;78(6):409–16.
- Kuhn AA, Doyle L, Pogoyan A, Yarrow K, Kupsch A, Schneider GH, et al. Modulation of beta oscillations in the subthalamic area during motor imagery in Parkinson's disease. *Brain* 2006a;129:695–706.
- Kuhn AA, Kupsch A, Schneider GH, Brown P. Reduction in subthalamic 8–35 Hz oscillatory activity correlates with clinical improvement in Parkinson's disease. *Eur J Neurosci* 2006b;23(7):1956–60.
- Kühn AA, Trottenberg T, Kivi A, Kupsch A, Schneider G-H, Brown P. The relationship between local field potential and neuronal discharge in the subthalamic nucleus of patients with Parkinson's disease. *Exp Neurol* 2005;194(1):212–20.
- Kühn AA, Tsui A, Aziz T, Ray N, Brücke C, Kupsch A, Schneider G-H, Brown P. Pathological synchronisation in the subthalamic nucleus of patients with Parkinson's disease relates to both bradykinesia and rigidity. *Exp Neurol* 2009;215(2):380–7.
- Lachaux J-P, Rodriguez E, Martinerie J, Varela FJ. Measuring phase synchrony in brain signals. *Hum Brain Mapp* 1999;8(4):194–208.
- Lempka SF, McIntyre CC, Maurits NM. Theoretical analysis of the local field potential in deep brain stimulation applications. *PLoS ONE* 2013;8(3):e59839.
- Levy R, Ashby P, Hutchison WD, Lang AE, Lozano AM, Dostrovsky JO. Dependence of subthalamic nucleus oscillations on movement and dopamine in Parkinson's disease. *Brain* 2002;125:1196–209.
- Little S, Beudel M, Zrinzo L, Foltynie T, Limousin P, Hariz M, et al. Bilateral adaptive deep brain stimulation is effective in Parkinson's disease. *J Neural Neurosurg Psychiatry* 2016;87(7):717–21.
- Little S, Pogoyan A, Neal S, Zavala B, Zrinzo L, Hariz M, et al. Adaptive deep brain stimulation in advanced Parkinson disease. *Ann Neurol* 2013;74(3):449–57.
- Lopez-Azcarate J, Tainta M, Rodriguez-Oroz MC, Valencia M, Gonzalez R, Guridi J, Iriarte J, Obeso JA, Artieda J, Alegre M. Coupling between beta and high-frequency activity in the human subthalamic nucleus may be a pathophysiological mechanism in Parkinson's disease. *J Neurosci* 2010;30(19):6667–77.
- Marceglia S, Mrakic-Spota S, Foffani G, Cogliamariani F, Caputo E, Egidi M, et al. Gender-related differences in the human subthalamic area: a local field potential study. *Eur J Neurosci* 2006;24(11):3213–22.
- Mraunkic-Spota S, Marceglia S, Egidi M, Carrabba G, Rampini P, Locatelli M, et al. Extracellular spike microrecordings from the subthalamic area in Parkinson's disease. *J Clin Neurosci* 2008;15(5):559–67.
- Nandi B, Swiatek P, Kocsis B, Ding M. Inferring the direction of rhythmic neural transmission via inter-regional phase-amplitude coupling (ir-PAC). *Sci Rep* 2019;9(1):6933.
- Nolte G, Bai Ou, Wheaton L, Mari Z, Vorbach S, Hallett M. Identifying true brain interaction from EEG data using the imaginary part of coherency. *Clin Neurophysiol* 2004;115(10):2292–307.
- Özkurt TE, Butz M, Homburger M, Elben S, Vesper J, Wojtecki L, Schnitzler A. High frequency oscillations in the subthalamic nucleus: a neurophysiological marker of the motor state in Parkinson's disease. *Exp Neurol* 2011;229(2):324–31.
- Priori A, Ardolino G, Marceglia S, Mrakic-Spota S, Locatelli M, Tamma F, Rossi L, Foffani G. Low-frequency subthalamic oscillations increase after deep brain stimulation in Parkinson's disease. *Brain Res Bull* 2006;71(1–3):149–54.
- Priori A, Egidi M, Pesenti A, Rohr M. Do intraoperative microrecordings improve subthalamic nucleus targeting in stereotactic neurosurgery for Parkinson's disease? *J Neurosurg Sci* 2003;47(1):56.
- Priori A, Foffani G, Pesenti A, Tamma F, Bianchi A, Pellegrini M, Locatelli M, Moxon K, Villani R. Rhythm-specific pharmacological modulation of subthalamic activity in Parkinson's disease. *Exp Neurol* 2004;189(2):369–79.
- Rampini PM, Locatelli M, Alimehmeti R, Tamma F, Caputo E, Priori A, et al. Multiple sequential image-fusion and direct MRI localisation of the subthalamic nucleus for deep brain stimulation. *J Neurosurg Sci* 2003;47(1):33–9.
- Ray NJ, Jenkinson N, Wang S, Holland P, Brittain JS, Joint C, Stein JF, Aziz T. Local field potential beta activity in the subthalamic nucleus of patients with Parkinson's disease is associated with improvements in bradykinesia after dopamine and deep brain stimulation. *Exp Neurol* 2008;213(1):108–13.
- Ray S, Maunsell JHR, Ungerleider L. Different origins of gamma rhythm and high-gamma activity in macaque visual cortex. *PLoS Biol* 2011;9(4):e1000610.
- Rodriguez-Oroz MC, Lopez-Azcarate J, Garcia-Garcia D, Alegre M, Toledo J, Valencia M, et al. Involvement of the subthalamic nucleus in impulse control disorders associated with Parkinson's disease. *Brain* 2011;134:36–49.
- Rosa M, Giannicola G, Marceglia S, Fumagalli M, Barbieri S, Priori A. Neurophysiology of deep brain stimulation. *Int Rev Neurobiol* 2012;107: 23–55.
- Rosa M, Marceglia S, Servello D, Foffani G, Rossi L, Sassi M, et al. Time dependent subthalamic local field potential changes after DBS surgery in Parkinson's disease. *Exp Neurol* 2010;222(2):184–90.
- Salimpour Y, Anderson WS. Deep brain stimulation therapy in Parkinson disease: the role of cortical phase-amplitude coupling reduction. *Neurosurgery* 2015;77(4):N17–9.
- Sanchez Bornot JM, Wong-Lin KongFatt, Ahmad AL, Prasad G. Robust EEG/MEG based functional connectivity with the envelope of the imaginary coherence: sensor space analysis. *Brain Topogr* 2018;31(6):895–916.
- Sanders TH. Phase-amplitude coupling, an indication of bursting in parkinsonism, is masked by periodic pulses. *J Neurophysiol* 2016;115(3):1587–95.
- Silberstein P, Kuhn AA, Kupsch A, Trottenberg T, Krauss JK, et al. Patterning of globus pallidus local field potentials differs between Parkinson's disease and dystonia. *Brain* 2003;126(12):2597–608.
- Sutton AC, Yu W, Calos ME, Smith AB, Ramirez-Zamora A, Molho ES, Pilitsis JG, Brochie JM, Shin DS. Deep brain stimulation of the substantia nigra pars reticulata improves forelimb akinesia in the hemiparkinsonian rat. *J Neurophysiol* 2013;109(2):363–74.
- Tort ABL, Kramer MA, Thorn C, Gibson DJ, Kubota Y, Graybiel AM, Kopell NJ. Dynamic cross-frequency couplings of local field potential oscillations in rat striatum and hippocampus during performance of a T-maze task. *Proc Natl Acad Sci U S A* 2008;105(51):20517–22.
- Tsiokos C, Malekmohammadi M, AuYong N, Pouratian N. Pallidal low beta-low gamma phase-amplitude coupling inversely correlates with Parkinson disease symptoms. *Clin Neurophysiol* 2017;128(11):2165–78.
- van Wijk BCM, Beudel M, Jha A, Oswal A, Foltynie T, Hariz MI, Limousin P, Zrinzo L, Aziz TZ, Green AL, Brown P, Litvak V. Subthalamic nucleus phase-amplitude coupling correlates with motor impairment in Parkinson's disease. *Clin Neurophysiol* 2016;127(4):2010–9.
- Vercruyse S, Spildooren J, Heremans E, Wenderoth N, Swinnen SP, Vandenberghe W, Nieuwboer A. The neural correlates of upper limb motor blocks in Parkinson's disease and their relation to freezing of gait. *Cereb Cortex* 2014;24(12):3154–66.
- Wang Q, Li M, Xie Z, Cai J, Li N, Xiao Hu, Wang N, Wang J, Luo F, Zhang W. Granger causality supports abnormal functional connectivity of beta oscillations in the dorsolateral striatum and substantia nigra pars reticulata in hemiparkinsonian rats. *Exp Brain Res* 2017;235(11):3357–65.
- Watson BO, Ding M, Buzsáki G. Temporal coupling of field potentials and action potentials in the neocortex. *Eur J Neurosci* 2018;48(7):2482–97.
- Weinberger M, Hutchison WD, Dostrovsky JO. Pathological subthalamic nucleus oscillations in PD: can they be the cause of bradykinesia and akinesia? *Exp Neurol* 2009;219(1):58–61.
- Yang AL, Vanegas N, Lungu C, Zaghoul KA. Beta-coupled high-frequency activity and beta-locked neuronal spiking in the subthalamic nucleus of Parkinson's disease. *J Neurosci* 2014;34(38):12816–27.